Drop Modulation by Second Harmonic Using Fresnel Lens in Acoustic Inkjet Printing

Toshinobu Hamazaki and Naoki Morita
RDC / DPC / Fuji Xerox Co., Ltd.
Ebina, Kanagawa, Japan

Abstract

Acoustic Inkjet Printing (AIP) is suitable for jetting a small drop when compared with other available methods because the drop size depends not on the nozzle area but on the frequency of acoustic beam that enables ejection from free liquid surface.

For inkjet printing, drop modulation is the major technology being effective to realize both high image quality and high print speed. In the previous reports regarding AIP, multiple droplets were fired at the same location on paper for gray scale of image.[1] This method could enhance image quality at the sacrifice of print speed.

Here we propose a method of drop size modulation in AIP to achieve both high image quality and high print speed. It has been proved that the drop size is modulated by a second harmonic on fresnel lens without changing the liquid level and other dimensions. This report also shows that calculations and experiments ascertained drop modulation by the second harmonic.

Introduction

Cross sections of AIP head structure and fabricated fresnel lens are shown in figures 1 and 2 respectively. A four-phase fresnel lens focuses an acoustic beam, which is radiated from the transducer, at free liquid surface to eject a drop.

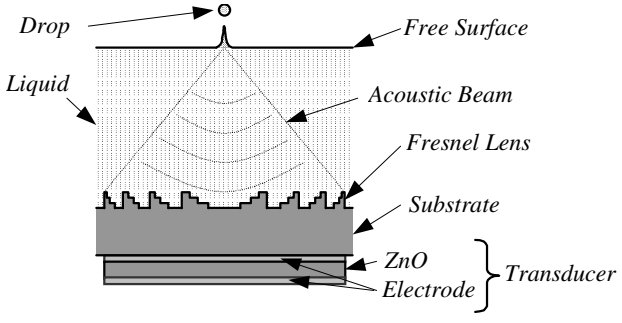

Figure 1. Schematic Cross Sections of Head Structure

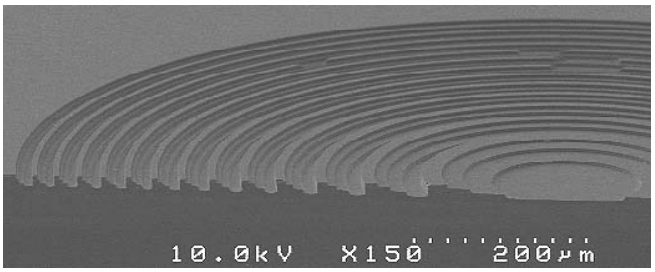

Figure 2. Fresnel Lens designed for 167 MHz

Burst wave is supplied to the transducer and its burst frequency, which is the frequency of plural sine waves in burst wave, decides the diameter of ejected drop.[2] Accordingly, jetting frequency depends on the cyclic frequency of burst waves. On the other hand, by using the fresnel lens, its focal distance becomes longer as the burst frequency is higher. Hence, drop modulation can be accomplished if the liquid level can be changed with the change of burst frequency. However it is almost impossible in actual print head control. For the reason, a second harmonic focus was considered for drop modulation without liquid level control, because the ultrasonic wave is focused by interference of wave based on Huygens' principle.

Sound field by fresnel lens was estimated from calculation using Rayleigh's Equation[3-5] and the characteristics of 2nd focus were predicted. Also experimental single lens devices were designed and fabricated to evaluate and understand the characteristics.

Design of Fresnel Lens

A four-phase fresnel lens is shown in figure 3. In the cylindrical coordinate $\boldsymbol{R}$ is the radial direction and $\boldsymbol{Z}$ is the axial direction. d_i is the height of each phase ring and R_n is the radius of each ring.

d_i and R_n are designed from equations (1) and (2) respectively, which are decided by the relationship of path distance and phase lag. Here, λ_l and λ_s are wavelength in liquid and solid respectively. l_d is a focal distance at a designed frequency f_d. Operating frequency f_d was selected to be 67, 83, 133 and 167 MHz and designed focal distance l_d was decided to be 1438 microns.

$$d_i = \frac{i}{4} \cdot \frac{1}{1/\lambda_l - 1/\lambda_s} \qquad (i=0,1,2,3) \tag{1}$$

$$R_n^2 = \left(l_d - d_3 + n \cdot \frac{\lambda_l}{4} \right)^2 - (l_d - d_3)^2 \quad (n=1,2,3,4,,,) \tag{2}$$

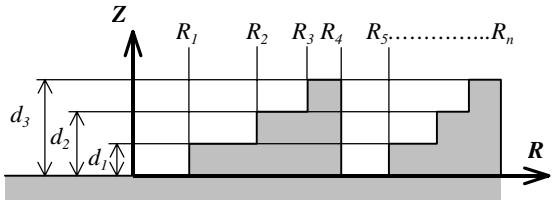

Figure 3. Cross Sections of Fresnel Lens

Calculation of Sound Field

The particle velocity v_T at the lens face in each phase is shown in equation (3) when a plane wave propagates in Si substrate. A and V_s are oscillation amplitude and sound velocity in solid respectively. Here Rayleigh's Equation was applied to fresnel lens and then equation (5) was obtained. p, ρ_l, S_T and V_l are sound pressure, density of liquid, lens area and sound velocity in liquid respectively.

p_N, a sound pressure normalized by p_0, is described as shown in equation (6) in consideration of ultrasonic attenuation in liquid. p_0 is a sound pressure at the lens bottom as shown in equation (4). k_l and k_s are wave numbers in liquid and solid respectively. α is an absorption coefficient which depends on the material itself at each ultrasonic frequency. The distribution of sound pressure around the fresnel lens was calculated by integrating equation (6) numerically.

$$v_T = A \exp\left[j\omega \left(t - d_i / V_s \right) \right] \tag{3}$$

$$p_0 = \rho_l V_l A \exp(j\omega t) \tag{4}$$

$$p = \rho_l \int_{S_T} \dot{v}_T \left(t - \frac{r}{V_l} - \frac{d_i}{V_s} \right) \frac{dS}{2\pi r} \tag{5}$$

$$p_N = jk_l \int_{S_T} e^{-jk_l r} e^{-jk_s d_i} e^{-\alpha r} \frac{dS}{2\pi r} \tag{6}$$

Sound fields were calculated in the case of water, ethanol and isopropyl alcohol (IPA) where the absorption coefficient and sound velocity vary widely as shown in table 1.[6]

Table 1. Absorption Coefficient and Sound Velocity at 20 degree C

	α / f^2 [neper/(m Hz^2)]	V_l [m/sec]
Water	2.6e-14	1482
Ethanol	5.2e-14	1182
IPA	9.2e-14	1170

Examples of calculated sound pressure are shown in figure 4. In this case, designed frequency of fresnel lens f_d is 133 MHz and liquid is water. Each line shows each case of different ultrasonic frequencies. The 1st focus by fundamental wave moves further from the lens and weakens its sound pressure as the acoustic frequency is higher. The 2nd focus by second harmonic appears at a closer position from the lens than the 1st focus in the case of higher frequency.

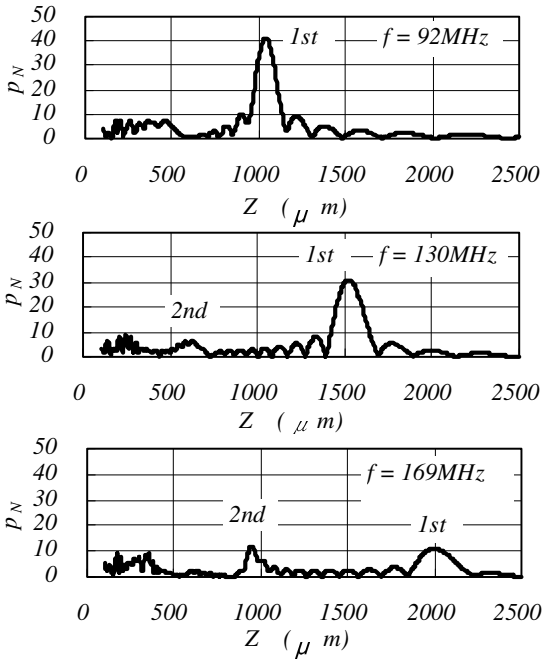

Figure 4. Calculated Sound Pressure on Z Axis

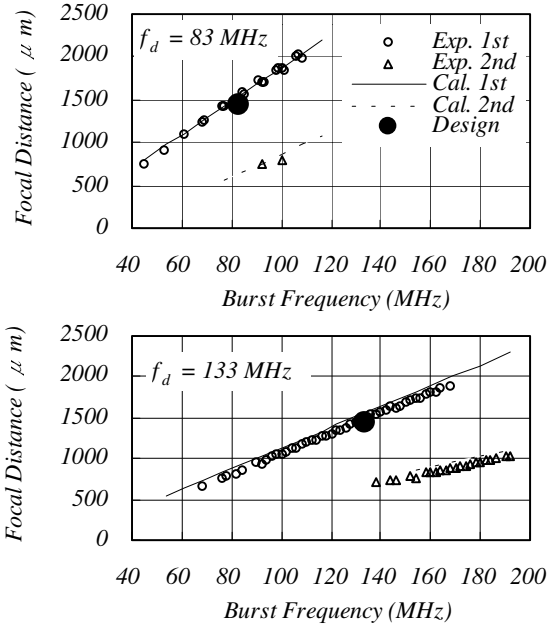

Figure 5. Calculated and Experimental Focal Distance

Results

Focal Distance

Experimental results of focal distance are compared to calculations with 83 and 133 MHz lenses in water as shown in figure 5. In this experiment, a focus point is defined as the center of area where a drop can be ejected at the fixed burst energy to the transducer. The 1st and 2nd foci depend on the burst frequency. Experimental results agree with calculations.

Energy for Drop Ejection

The RF burst energy, which is fixed by burst amplitude and burst length, is supplied to the transducer for drop ejection. In figures 6 and 7, calculations and experiments examined the relation between drop ejection and burst length at fixed burst amplitude. Fluid dynamics software 'FLOW-3D' was used for calculations where the body force was supplied at focus area in liquid during the burst length.

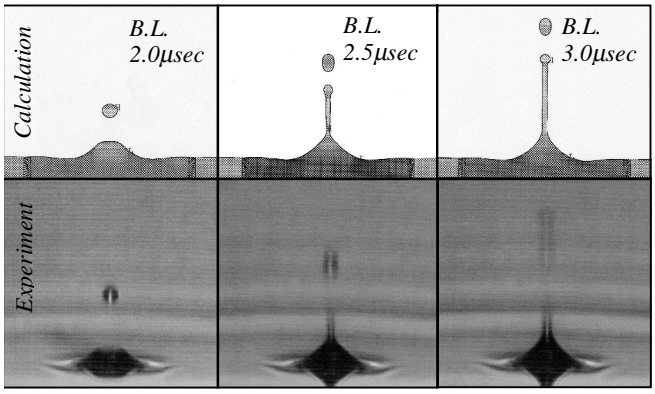

Figure 6. Drop Ejection of Calculations and Experiments

One drop can be separate from free liquid surface when burst energy exceeds the threshold. As the burst length is longer, a long liquid column is ejected and then the column separates to plural drops as shown in figure 6. The dependency of drop ejection on the burst length has good agreement between calculations and experiments as shown in figure 7 where the body force is adjusted to agree on the drop velocity.

The energy threshold of drop ejection is supposed to depend on the sound pressure at the focus, kinetic energy of ejected drop and surface tension of ink. The following is the comparison between calculated sound pressure and experimental energy threshold of drop ejection at the 1st focus. In this experiment, energy threshold is defined by burst length at fixed burst amplitude when a drop is separated from free liquid surface.

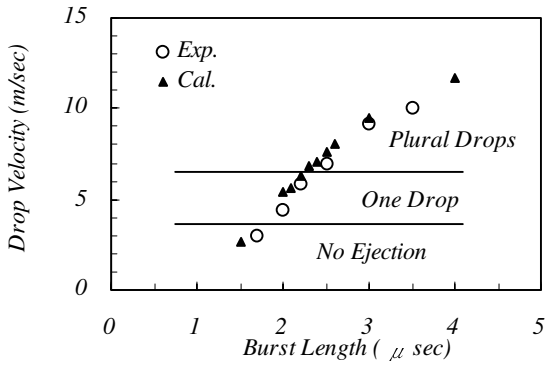

Figure 7. The Dependency of Drop Ejection on Burst Length

In case of 133 MHz lens, calculated sound pressure at the 1st focus is shown in figure 8 and experimental energy threshold of drop ejection at the 1st focus is shown in figure 9 with three test liquids as shown in table 1. In case of water, calculated sound pressure and experimental energy threshold are shown in figures 10 and 11 respectively with four test lens types.

Normalized sound pressure in each liquid and each lens shows a maximum point in burst frequency. Also energy threshold shows a minimum point in burst frequency. These characteristics on calculations and experiments are similar dependency dominated by burst frequency, liquids and lenses because it is predictable that the energy threshold becomes lower when the normalized sound pressure at focus is higher.

Drop Volume and Drop Velocity

The dependency of drop volume and velocity on the burst frequency is shown in figures 12 and 13 respectively where a drop of water was ejected by 133 MHz lens at fixed burst energy. The drop volume becomes smaller when the burst frequency is higher and the burst energy is lower. The drop volume by the 2nd focus also exists on the same curve by the 1st focus. The drop velocity by the 1st and 2nd foci shows a maximum point at each certain frequency, probably because the drop velocity is decided by the sound pressure at focus shown in figure 8.

Drop Modulation

Drop modulation using 133 MHz lens with water is shown in figure 14. Drops of different size could be ejected at fixed liquid surface by level control when an adequate liquid level for both the 1st and 2nd foci was chosen in figure 5. The liquid level from the lens bottom was 989 microns. Big drop of 4.8 pl and small drop of 1.2 pl were ejected by burst frequency at 92 and 177 MHz respectively as shown in (a) and (b). Burst energy was adjusted to eject one stable drop in each case because if applied energy is not within an adequate range, plural drops or an unstable weak drop are ejected, causing print defects.

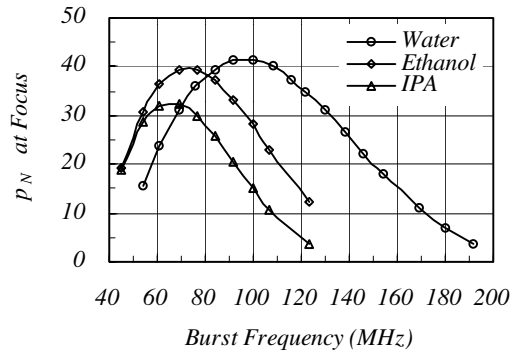

Figure 8. Calculated Sound Pressure

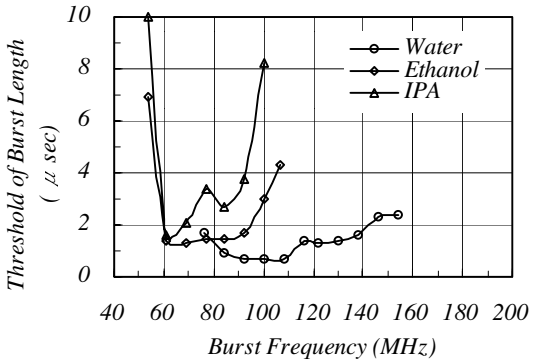

Figure 9. Experimental Energy Threshold

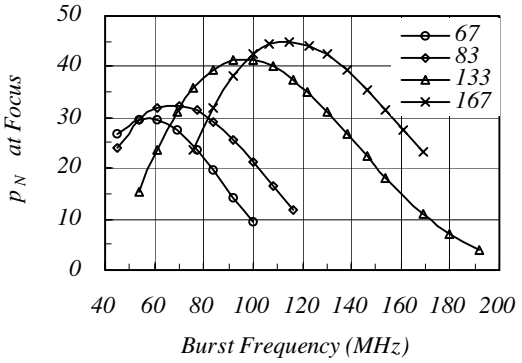

Figure 10. Calculated Sound Pressure

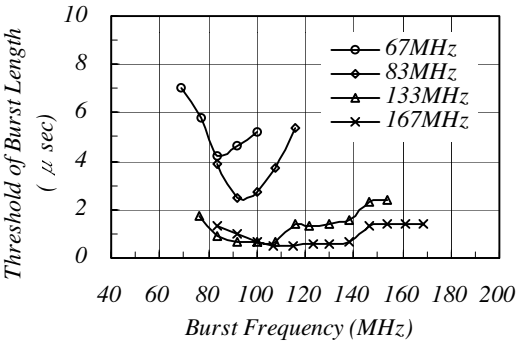

Figure 11. Experimental Energy Threshold

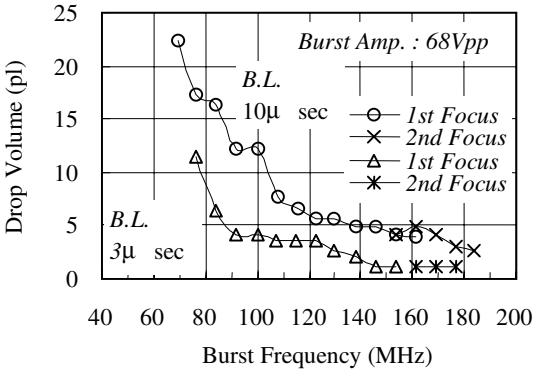

Figure 12. Dependency of drop volume on burst frequency.

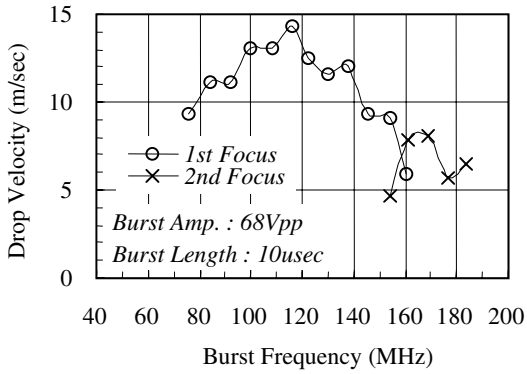

Figure 13. Dependency of Drop Velocity on Burst Frequency

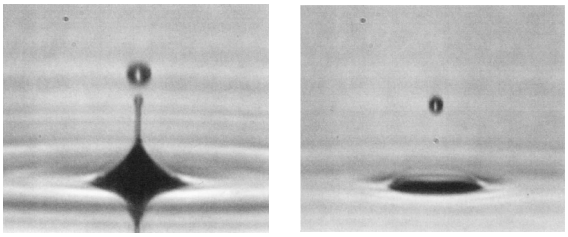

(a) *(b)*

Figure 14. Drop size modulation by Burst Frequency Optimization

Conclusion

Drop modulation at fixed liquid surface in acoustic inkjet printing using a four-phase fresnel lens was predicted by calculations and proved by experiments. These results contribute to the enhancement of image quality without sacrificing print speed in AIP. Calculations using Rayleigh's Equation showed good agreement with experiments on the focal distance and energy threshold. Accordingly, the methods would enable designing guideline for fresnel lens.

References

1. B. Hadimioglu, S. A. Elrod, Martin Lim,
2. D. L. Steinmetz, J. C. Zesch, B. T. Khuri-Yakub, E. G. Rawson and C. F. Quate, Acoustic Ink Printing : Printing by Ultrasonic ink Ejection, *IS & T's NIP 8*, pg. 411, 1992.
2. S. A. Elrod, B. Hadimioglu, B. T. Khuri-Yakub, E. G. Rawson, E. Richley and C. F. Quate, Nozzleless droplet formation with focused acoustic beams, J. Appl. Phys. 65 (9), 1 May 1989.
3. J.W.S. Rayleigh, *The Theory of Sound*, Vol.2, p.107, Dover Publications, New York, 1945.
4. S. Ohtsuki, Calculation Method for the Nearfield of a Sound Source with Ring Function, *J. Acoustical Society of Japan*, Vol **30**, No.2, pg. 76, 1974.
5. S. Ohtsuki, Calculation Technique of Sound Field and Its Visualization, *J. Acoustical Society of Japan*, Vol **54**, No.2, pg. 140, 1998.
6. Handbook of Ultrasonic wave in Japanese, Maruzen, pg. 714, 1999.

Biography

T. Hamazaki graduated from department of mechanical engineering, Tokyo Institute of Technology and joined Fuji Xerox in 1991. He was engaged in research and development on thermal inkjet and acoustic inkjet. Especially his interests are print head design, evaluation of jetting characteristics, modeling of jetting and computational fluid dynamics. He contributed to the products of thermal inkjet printer from Fuji Xerox in 1998.